






Article

# The Petunia CHANEL Gene is a ZEITLUPE Ortholog Coordinating Growth and Scent Profiles

Marta I. Terry <sup>1</sup>, Fernando Pérez-Sanz <sup>2</sup>, M. Victoria Díaz-Galián <sup>1</sup>, Felipe Pérez de los Cobos <sup>3</sup>, Pedro J. Navarro <sup>4</sup>, Marcos Egea-Cortines <sup>1</sup> and Julia Weiss <sup>1,\*</sup>

<sup>1</sup> Genética Molecular, Instituto de Biotecnología Vegetal, Edificio I+D+I, Plaza del Hospital s/n, Universidad Politécnica de Cartagena, 30202 Cartagena, Spain; marta.terry@edu.upct.es (M.I.T.); mariavictoria.diaz@edu.upct.es (M.V.D.-G.); Marcos.Egea@upct.es (M.E.-C.)

<sup>2</sup> Biomedical Informatic and Bioinformatic Platform, Biomedical Research Institute of Murcia, University Clinical Hospital 'Virgen de la Arrixaca', University of Murcia, 30120 Murcia, Spain; fernando.perez8@um.es

<sup>3</sup> Plant Breeding Department, Center of Edafology and Applied Biology of Segura-High Council for Scientific Research (CEBAS-CSIC), Espinardo University Campus, Espinardo, 30100 Murcia, Spain; fpcobos@cebas.csic.es

<sup>4</sup> Escuela Técnica Superior de Ingeniería de Telecomunicación (DSIE), Campus Muralla del Mar, s/n., Universidad Politécnica de Cartagena, 30202 Cartagena, Spain; pedroj.navarro@upct.es

\* Correspondence: Julia.weiss@upct.es; Tel.: +34-968-325-777

Received: 4 March 2019; Accepted: 9 April 2019; Published: 11 April 2019



**Abstract:** The floral perianth, comprising sepals and petals, conceals the sexual organs and attracts pollinators. The coordination of growth and scent emission is not fully understood. We have analyzed the effect of knocking down *CHANEL* (*PhCHL*), the *ZEITLUPE* ortholog in petunia (*PhCHL*) by hairpin RNAs. Plants with low *PhCHL* mRNA had overall decreased size. Growth evaluation using time lapse image analysis showed that early leaf movement was not affected by *RNAi:PhCHL*, but flower angle movement was modified, moving earlier during the day in knockdown plants than in wild types. Despite differences in stem length, growth rate was not significantly affected by loss of *PhCHL*. In contrast, petal growth displayed lower growth rate in *RNAi:PhCHL*. Decreased levels of *PhCHL* caused strongly modified scent profiles, including changes in composition and timing of emission resulting in volatile profiles highly divergent from the wild type. Our results show a role of *PhCHL* in controlling growth and development of vegetative and reproductive organs in petunia. The different effects of *PhCHL* on organ development indicate an organ-specific interpretation of the down regulation of *PhCHL*. Through the control of both timing and quantitative volatile emissions, *PhCHL* appears to be a major coordinator of scent profiles.

**Keywords:** floral scent; petal development; growth rate; phenomics; circadian clock; *ZEITLUPE*; image analysis; hairpin RNA

## 1. Introduction

Plant aerial organs grow from lateral primordia that form in the shoot apical meristem [1]. The type of organs produced, i.e., leaves or flowers, are the result of a vegetative or reproductive developmental program. The formation of flowers is the result of the activation of the so-called floral organ identity genes. They comprise a set of MADS-BOX proteins that in a combinatorial fashion allow the formation of the different organs [2]. The interaction of different MADS-box proteins occur via formation of protein complexes that activate the different organ identity programs leading to the formation of sepals and petals in the perianth and stamens and carpels [3,4].

Floral organs play an important role in reproductive success in many plants. Proper floral size is a key component of flower-pollinator interaction [5]. Floral size, like in leaves, is controlled by coordinated cell division and expansion processes [6]. The genes controlling lateral organ size appear to be conserved. Indeed, general regulators of lateral growth such as *AINTEGUMENTA* control floral size in *Arabidopsis*, *petunia*, *Antirrhinum* and tobacco [7–9].

During late flower development and maturation there is a major transcriptional reprogramming and scent emission starts with flower opening [10,11]. Scent emission takes place when the floral organ identity genes are not fully active, indicating a quantitative effect of the *DEFICIENS/GLOBOSA* MADS box proteins and downstream factors on scent emission [11].

There are a large number of plants that emit floral volatiles with significantly larger outputs during the day or during the night [12–16], suggesting a circadian regulation of scent emission. The circadian clock genes *LATE ELONGATED HYPOCOTYL* in *petunia* (*PhLHY*) and *NaLHY* and *ZEITLUPE* (*NaZTL*) in *Nicotiana attenuata* have been investigated and control the timing of emission of methyl benzoate and benzyl benzoate in *petunia* and benzyl acetone in *N. attenuata* [17,18]. Thus, a default pathway controlled by petal identity may activate floral scent emission, and the fine tuning in terms of emission timing should be regulated by the clock. However, this emerging hypothesis requires further experimental support; the studies mentioned have analyzed a small number of volatile organic compounds (VOCs), but the effect, if any, of the circadian clock on scent profiles is not known.

In this work, we have analyzed the down-regulation of the *petunia* gene ortholog of *ZTL* and its effect on growth and scent emission. We found that *PhZTL* plays a differential role in stem and floral size and is a major coordinator of floral scent profiles in *petunia*. As a result, we named the gene *CHANEL* (*PhCHL*).

## 2. Materials and Methods

### 2.1. Gene Identification and Phylogenetic Analysis

We identified *ZTL* orthologs and paralogs in the *Petunia* genome using BLAST [19]. The identified scaffolds and cDNAs were used to confirm the genome annotation using Genewise [20]. Protein alignment was performed with CLUSTALX [21]. Phylogenetic analysis was performed with the R libraries *ape* and *phangorn* [22,23], using the Maximum Likelihood as statistical method, JTT (Jones, Taylor and Thornton) as model of amino acid substitution, and 1000 bootstrap replicates. Trees were visualized and annotated with *ggtree* [24] using R, (R version 3.5.1). Protein accessions are listed in Table S1.

### 2.2. Silencing of *PhCHL*

We obtained sequence information from the genomic clone of *PhCHL* (Peaxi162Scf01124g00126.1) found in W115 (or Mitchell) and amplified 255 bp encompassing the last nine coding codons and 3' untranslated region. As the major effect of silencing of *ZTL* in *petunia* was a major disruption of scent profiles, we called it *CHANEL*, a famous perfume. The specific sequence of *PhCHL* was:

```
>PhCHL
TGAACATCTTTAGCAAGCTCTGTCATTTGAATAAAGAAAAAGTAATGATGAAGAGAAG
GTGTTGTGCAGTATTCATAATGAAAATTTTGCCTCAAGAATAAAGAGAGTCCCGAGCAAAC
TTGCAGTGCAGTTTTTGCATTGCACCAATGCATAAATGACTAGCAAGTACCTGTGAGTTAGTG
GCTGTCTTGTATTCTTGTGTGGCTCATATGCCATGGTGAGCAAATGGTCCTATTGAGCAGATG
GTC
```

We used primers, introducing a partial *attb1* and *attb2* recombination site for GATEWAY cloning using *PhCHL**rnaiaattb1* and *PhCHL**maiattb2* (Table S2). We performed a second PCR using *attb1* and *attb2* to add the corresponding sequences for recombination. The amplified fragment was recombined into pDONR221 and into the GATEWAY vector pHELLSGATE12 to obtain a hairpin construct [25]. The pHELLSGATE12 drives the hairpin construct using a standard 35S promoter. The W115 Mitchell double haploid was transformed as described previously [7].

Transformed plants were identified by PCR with primers amplifying NPTII. The completeness of the construct was tested with the Agri 51 and Agri 56 primers [26] (see Table S2). The PCR conditions were 3 min at 95 °C followed by 35 cycles of 15 s at 95 °C, 15 s at 55 °C and 15 s at 72 °C, and terminated by 5 min at 72 °C (Kapa Biosystems). The PCR reactions were loaded on 1% agarose gel containing ethidium bromide. PCR products from T2 plants were purified and sequenced.

### 2.3. Plant Growth Conditions and Sampling

Petunia plants were grown using a commercial substrate in a greenhouse under natural conditions. All experiments were conducted with at least three biological replicates. To study the expression of *PhCHL*, non-transgenic siblings and two independent *RNAi:PhCHL* T2 lines (*RNAi:PhCHL3* and *RNAi:PhCHL10*) were transferred to a climate chamber with 12 h of light and 12 h of dark (12LD) or 8L:16D and 23 °C and 18 °C for day and night, respectively. Plants were acclimated for 4–5 days. Young leaves and petals from 2–3 day-old flowers were sampled every three h for 24 h; tissues were immediately frozen in liquid nitrogen and stored at -80 °C until further analysis.

To analyze the floral scent of non-transgenic and transgenic petunia flowers, we took at least three biological replicates of 2–3 day-old flowers (one flower per plant) every three h.

### 2.4. Housekeeping Genes and Gene Expression Analysis by qPCR

RNA was extracted from three biological replicates per time point of leaves and corollas using acid phenol [27]. Concentrations were measured using NanoDrop (Thermo-Fisher). Equal amounts of total RNA were used to obtain cDNA using Maxima kits (Thermo-Fisher) according to the user manual.

Previously, we performed a study to validate the housekeeping gene or genes, in two tissue samples, petal and leaf, for time course studies according to [28]. The candidate genes were *ACTIN 11* (*ACT*), *CYCLOPHILIN* (*CYP*), *ELONGATION FACTOR 1 $\alpha$*  (*EF1 $\alpha$* ), *GLYCALDEHYDE-3-PHOSPHATE DEHYDROGENASE* (*GADPH*), *RIBOSOMAL PROTEIN S13* (*RPS13*), *GTP-NUCLEAR BINDING PROTEIN* (*RAN1*) and *POLYUBIQUITIN* (*UBQ*) (Table S2). PCR analysis was performed as described previously [28]. The following protocol was used for 40 cycles: 95 °C for 5 s, 60 °C for 20 s and 72 °C for 15 s (Clontech SYBR Green Master Mix and Mx3000P qPCR Systems, Agilent Technologies), samples were run in duplicate. Cycle threshold (Ct) values were analyzed by BestKeeper [29], NormFinder [30], geNorm [31] and comparative  $\Delta$ Ct methods [32] implemented in the web-based tool RefFinder [33] at different time points (Figure S1).

Analyzing all tissues, the most stable genes were *PhCYP* and *PhEF1 $\alpha$*  (Figure S2A). Moreover, for individual tissues, results were slightly different: the best genes for normalization in leaves were *PhACT* and *PhEF1 $\alpha$* , and for petals, *PhACT* and *PhCYP* (Figure S2B,C).

We used *PhACT* to normalize the expression of clock genes in petunia leaves and petals as described [34]. Normalized expression was calculated as described [34] using the REST program [29] and *PhACT* as internal control gene.

Primers for circadian clock genes were designed using pcrEfficiency [35] (Table S2) and the following protocol was used for 40 cycles: 95 °C for 5 s, 60 °C for 20 s and 72 °C for 15 s. Samples were run in duplicate. Primer combinations were tested with genomic DNA from Mitchell, and we found that all of them gave a single copy DNA on agarose gels. The endpoint PCR was further verified by melting point analysis where all primer combinations gave a single peak of melting (Figure S3).

### 2.5. Image Acquisition

We used an image acquisition system described previously [36]. Plants were grown inside a growth chamber comprising LED lights covering from UV to red light. Day and night images were taken by activating an Infrared light at 840 nm wavelength during short intervals of time (3 s). Images were acquired every ten minutes with an artificial vision camera comprising two CCD sensors, a multichannel 24-bit RGB absorbing at 610 nm, 540 nm and 460 nm, and a monochromatic sensor capturing at 800 nm. The acquired images have a resolution of 1296 × 966 pixels.

We obtained data using transgenic lines and compared them to the segregating siblings. Leaf growth and movement in seedlings was recorded for a period of 12 days with a total of 1728 images. Stem and flower growth was recorded for a period of 5 days and 16 h for line 3 and 3 days for line 10, for a total of 822 images and 432 images respectively. Using a semi-automatic procedure, we measured the length and angle of the longitudinal axis as referred to the horizontal plane of the flowers, as well as the length of the stem. The acquisition intervals were 1 hour for line 3 and 2 h for line 10, to explore differences in flower and stem growth patterns between wild-type and transgenic individuals. Analysis of growth was performed using the R package *grofit* [37]. Graphics were done using the color-blind friendly palette.

### 2.6. Scent Analysis

Flowers were placed in a glass beaker with a solution 4% of glucose inside a desiccator. Emitted volatiles were collected with twisters from the headspace every three h and analyzed by GM/CS as described [16]. Total and relative amounts were calculated using total integrated area divided by fresh weight as described before [38]. Detection of rhythmic scent emission was performed using the JTK\_CYCLE algorithm [39] implemented in the R package *MetaCycle* [40]. Scent profile figures were plotted using the R library *ggplot2* [41], using color palettes providing by the package *viridis* [42].

## 3. Results

### 3.1. The *Petunia* Genomes Have a Single ZTL Gene

We mined the *petunia* genomes to identify ZEITLUPE/FLAVIN-BINDING KELCH REPEAT F-BOX (ZTL/FKF) orthologs and paralogs using BLAST. We found two genes with homology to the Arabidopsis genome in *P. axillaris*: Peaxi162Scf01124g00126.1 and Peaxi162Scf00655g00114.1; and three in *P. inflata*: Peinf101Scf01230g02037.1, Peinf101Scf02808g00015.1 and Peinf101Scf04186g00007.1 (Table S3).

We performed a phylogenetic reconstruction of the genes found in *petunia* and compared them to the LOV-F-box-KELCH proteins from several monocots, dicots and the basal plant *Marchantia polymorpha* (Figure S4). As previously mentioned, the silencing of *PhCHL* caused a major change in the composition of floral scent. Thus, we named the gene CHANEL (*PhCHL*) (see below).

The phylogenetic reconstruction shows two major clades, one containing all the FKF)-like genes and a second one comprising the ZTL and the Arabidopsis LOV KELCH PROTEIN2 (LKP2). In both clades, two subclades separate monocots from dicots. The *Marchantia* FKF like gene [43] falls somewhere between the FKF group of coding genes and the ZTL coding set of genes. The genomes of *P. axillaris* and *P. inflata* appear to have one gene corresponding to *PhCHL*, but differ in the copy number of FKF that is found in two copies in *P. inflata*. According to the ancestral region by gene analysis of *Petunia hybrida* W115, the ZTL-FKF genes present in *P. hybrida* correspond to *P. axillaris* [19]. Thus, based on the phylogenetic reconstruction, we identified Peaxi162Scf01124g00126.1 as *PhCHL* and Peaxi162Scf00655g00114.1 as *PhFKF*.

### 3.2. The Expression of *PhCHL* is Organ Specific and Affected by Day Length

The *PhCHL* expression has been studied in leaves and seedlings of *Nicotiana attenuata* and Arabidopsis [17,44,45]. In these plants and tissues, *PhCHL* does not show rhythmic expression. We determined the set of reference genes for circadian expression in leaves and petals in order to establish the circadian gene expression patterns in *petunia* (see Materials and Methods). We analyzed the expression of *PhCHL* in *petunia* corolla using a 12:12 LD light regime and found that the expression had its maximum at ZT9 (Figure 1A). We found that the expression at ZT9 was significantly higher, and the lowest expression occurred at ZT15. Although the expression of *PhCHL* in corollas showed a peak at ZT9, the mathematical analysis for circadian oscillation using the JTK\_CYCLE algorithm indicated that the expression of *PhCHL* in *petunia* corollas was not rhythmic ( $p = 1$ ). We also analyzed the expression of *PhCHL* in leaves and the pattern was similar to corollas: *PhCHL* increased at ZT9

(Figure 1A), and its expression was not rhythmic ( $p = 1$ ). Under short days (8L:16D), the expression of *PhCHL* in leaves reached its maximum at midnight (ZT17) while the maximum expression in petals was detected during the afternoon (ZT5) (Figure 1B). As observed under 12L:12D, *PhCHL* did not display a rhythmic expression either in leaves or petals ( $p > 0.05$ ).

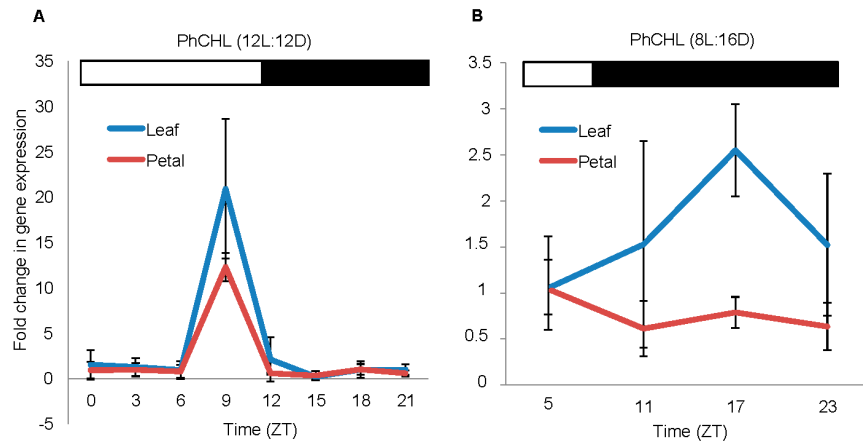


**Figure 1.** *PhCHL* expression in W115 petunia under 12LD (A) and 8L16D cycle (B) in leaves (blue line) and petals (red line) revealed a different pattern depending on light conditions. The maximum expression occurred before the dark period (ZT9) in leaves and petals under a 12LD cycle (A). This maximum was delayed in leaves under short days. *PhCHL* maintained its peak before dusk in petals (B). Results represent average  $\pm$  standard deviation from three replicates. White bar indicates the light period and black bar, the dark period.

### 3.3. Silencing *PhCHL* Does Not Affect *PhFKF*

We knocked down *PhCHL* using a RNAi hairpin construct and found significant down regulation of *ZTL* in several lines. We used two lines for further analysis. *RNAi:PhCHL10* showed a down regulation of 80% ( $p = 0.032$ ), while *RNAi:PhCHL3* showed a downregulation of 68% ( $p = 0.047$ ) (Figure 2A). We also analyzed the expression of FLAVIN-BINDING KELCH REPEAT F-BOX 1 (*PhFKF*), to discard co-silencing of the paralogous genes (*ZT5*). The expression of *PhFKF* did not differ significantly between transgenic and non-transgenic petunias (Figure 2B).

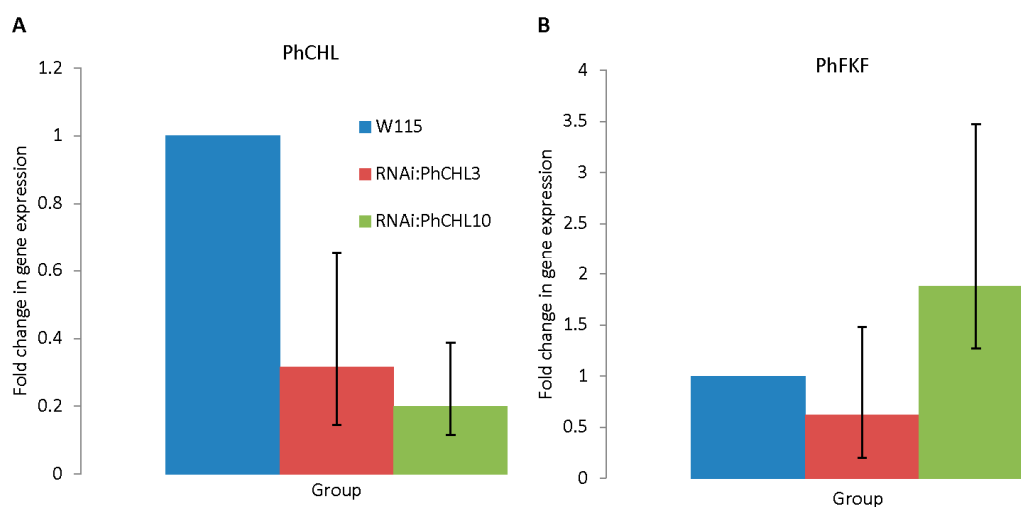


**Figure 2.** *PhCHL* (A) and *PhFKF* (B) expression in wild-type (blue bar) and *RNAi:PhCHL* plants (red bar and green bar) petals. *PhCHL* expression was significantly down-regulated in *RNAi:PhCHL3* ( $p = 0.047$ ) and *RNAi:PhCHL10* ( $p = 0.032$ ) compared to the wild-type (A). Silencing *PhCHL* did not affect *PhFKF* expression *RNAi:PhCHL3* ( $p$  value = 0.6), *RNAi:PhCHL10* ( $p$  value = 0.06) (B).



### 3.4. *PhCHL* Is a Positive Regulator of Lateral Organ Growth

We quantified the effect of *RNAi:PhCHL* on plant development and found that while not all parameters analyzed showed statistically significant changes, in general terms, *PhCHL* appears to play a role in the production of above ground biomass affecting organ size (Table 1). Thus, *RNAi:PhCHL* plants were significantly shorter than the non-transgenic siblings by roughly 23%. We analyzed floral size by measuring the length of the tube and the maximum expansion of the limb and found that, while the tube length was not always affected, the limb expansion was significantly reduced by *RNAi:PhCHL*, with size changes in the range of 12–18% (Table 1). Finally, we did not find differences in chlorophyll content (Table 1) or in the general canopy architecture i.e., number of branches (data not shown).

**Table 1.** Phenotypic analysis of *RNAi:PhCHL* lines 3 and 10 and comparison to non-transgenic siblings in T2 generation. Plant height, floral limb and floral tube length were measured from *RNAi:PhCHL* lines (3, 10) and the wild-type W115. Results, in centimeters, represent average  $\pm$  standard deviation. *p*-value  $< 0.05$  indicates a significant difference between non-transgenic and transgenic plants, significance levels are indicated with one asterisks (\* for  $p < 0.05$ ), two asterisks (\*\* for  $p < 0.001$ ) and three asterisks (\*\*\*) for  $p < 0.0001$ . NS indicates not significant differences.

| Measure      | RNAi:PhCHL       |                  | W115             | p-Value     |              |
|--------------|------------------|------------------|------------------|-------------|--------------|
|              | Line 3           | Line 10          |                  | RNAi:PhCHL3 | RNAi:PhCHL10 |
| Plant height | 25.1 $\pm$ 1.89  | 21.7 $\pm$ 4.18  | 37.33 $\pm$ 3.0  | 0.07        | 0.022 *      |
| Floral limb  | 4.37 $\pm$ 0.44  | 4.76 $\pm$ 0.55  | 5.38 $\pm$ 0.29  | 0.00009 *** | 0.0038 **    |
| Floral tube  | 4.07 $\pm$ 0.37  | 4.81 $\pm$ 0.51  | 4.82 $\pm$ 0.35  | 0.00055 *** | NS           |
| Chlorophyll  | 39.43 $\pm$ 6.32 | 36.65 $\pm$ 9.77 | 39.30 $\pm$ 9.80 | NS          | NS           |

We can conclude that *RNAi:PhCHL* is a positive regulator of lateral organ size with a pleiotropic effect causing a decrease in shoot and flower size.

### 3.5. *PhCHL* Is Involved in Flower Angle Changes but Not Leaf Movement

As size was negatively affected by *RNAi:PhCHL* (Table 1), we used a phenomics approach with time lapse image acquisition to identify the effects on growth kinetics [46]. We tried to analyze leaf growth in seedlings; however, leaf movement, a trait under light and circadian control, was so extreme that we could not obtain reliable data for growth (Movie S1). Changes in leaf position appeared to correspond to day/night changes. We measured the changes in leaf position every hour for a period of four days. We found that both non-transgenic and transgenic lines had open leaves during the day and closed leaves during the night (Movie S1). The changes in leaf opening and closing, in terms of speed or timing were not affected by the *PhCHL* expression levels (Figure 3A). Indeed, a mathematical analysis of the period, lag phase and amplitude did not show significant differences between *RNAi:PhCHL* and wild type (Table S4).

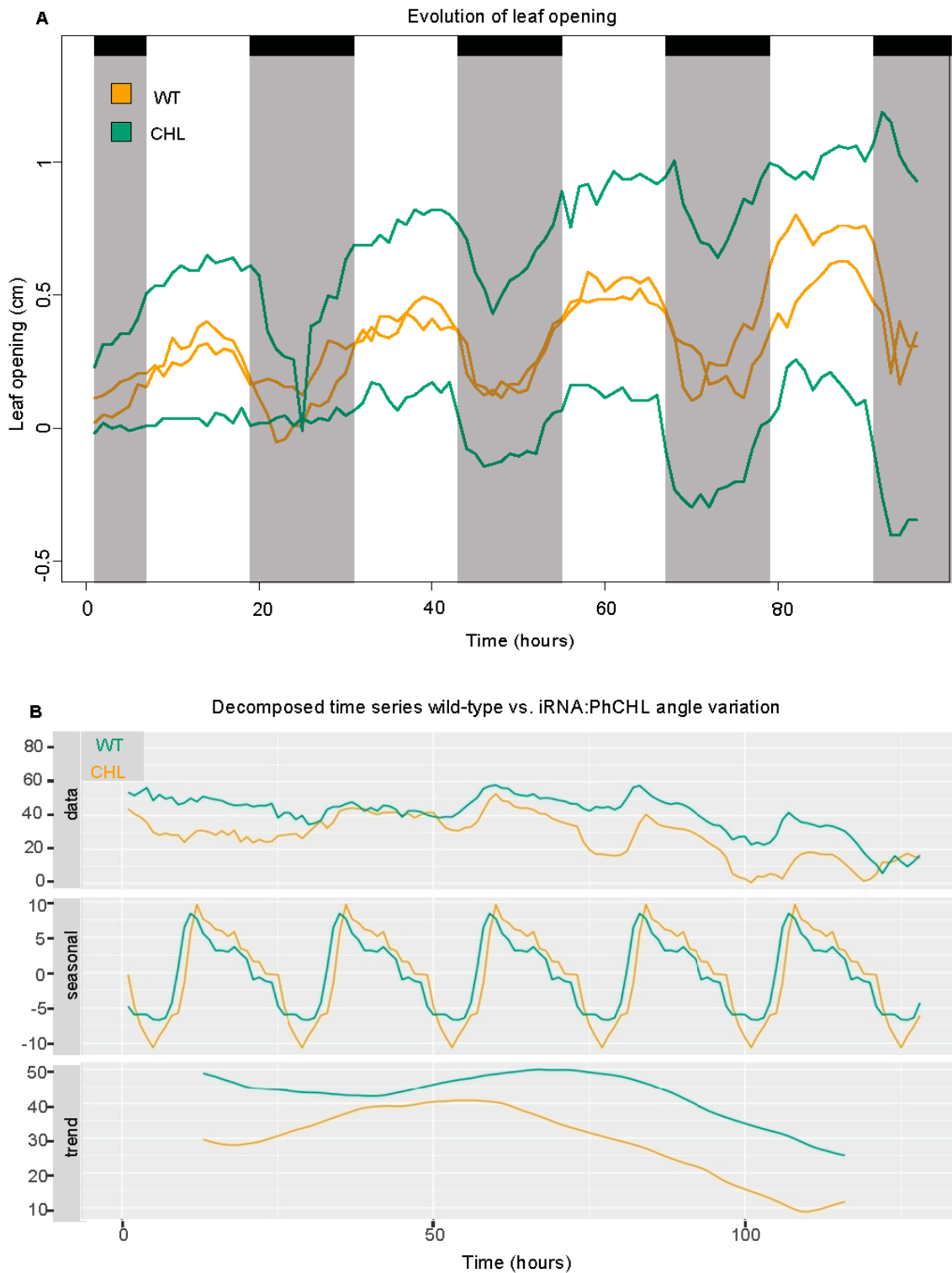


**Figure 3.** Down regulation of *PhCHL* does not affect leaf movement (A) The distance between the center of the plant and the end of each leaf is shown. Furthermore, these data correspond to the distance in the X axis. Negative values correspond to leaf positions where the tip of the leaf passed the center of the plant. Down regulation of *PhCHL* causes increased flower angles and advanced daily changes (green line, B). Orange line represents WT plants, green line represents *RNAi:PhCHL* plants.

We analyzed flower angle against the horizontal axis, as it is a parameter related to pollination that is regulated by *NaZTL* in *Nicotiana attenuata* [17]. Both wild-type and transgenic lines had a similar

daily pattern of flower movement; however, RNAi line 3 flowers had always higher angles than the non-transgenic siblings. A decomposed time series showed that their daily changes in angle were slightly advanced compared to wild type (Figure 3B).

### 3.6. Differential Effect of *PhCHL* on Stem and Flower Growth Rate

The difference in overall plant size indicated a role of *PhCHL* in plant growth. We analyzed stem growth and found that growth curves (Table 2) were similar in wild-type and transgenic plants (Figure 4A; Table 2). Still, maximal growth speed in transgenic line 3 was 80.7% compared to wild type and area under the curve was 82%. The data indicates that stems are shorter because growth occurs during shorter periods of time, but growth speed appears to be less affected in the stem (see discussion).

**Table 2.** Growth rate of petunia stems and flowers. Maximal growth is expressed in mm. Stems grew from day 0 and total growth refers to size achieved after 5 days and 16 h taking as reference the stem at time zero. Maximum growth for flowers refers to the same period but comprises the overall floral size. The maximum slope depicts growth rate while the area under the model (integral) gives an estimation of the overall difference in accumulated growth.

| Group             | Rate          | Max.Growth/Std.Error | Max.Slope/Std.Error | Area under Model |
|-------------------|---------------|----------------------|---------------------|------------------|
| WT                | Stem growth   | 16.084/0.142         | 0.121/0.005         | 1778.3           |
| <i>RNAi:PhCHL</i> | Stem growth   | 12.984/0.096         | 0.118/0.006         | 1471.53          |
| WT                | Flower growth | 57.698/0.403         | 0.798/0.013         | 3598.88          |
| <i>RNAi:PhCHL</i> | Flower growth | 39.677/0.344         | 0.566/0.011         | 2328.95          |



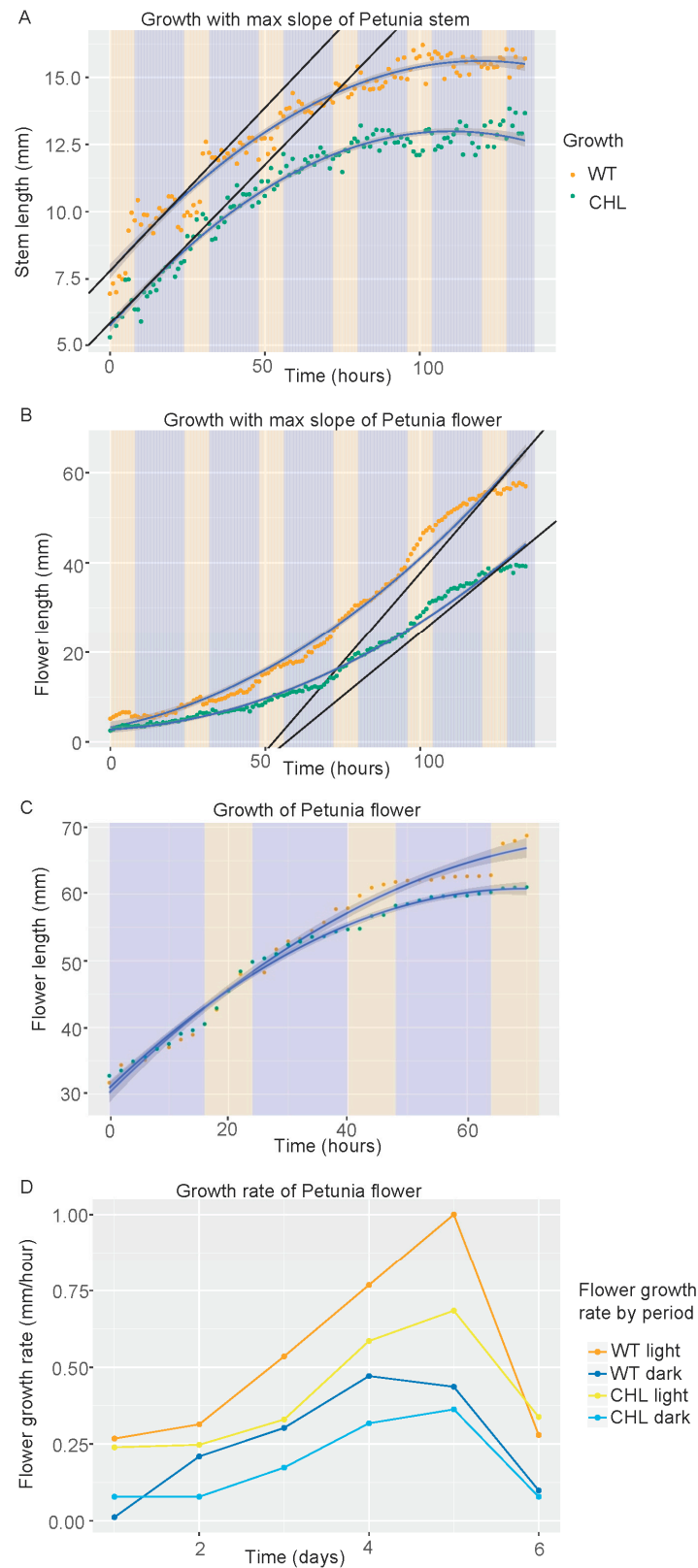


**Figure 4.** Down regulation of *PhCHL* affects growth length in stems (A) and growth rate in flowers (B,C). Graphics show the raw data (points), the adjusted curve and confidence interval (grey shade). Orange line represents WT plants, green line represents *RNAi:PhCHL* plants. Yellow and blue areas indicated light and dark period, respectively. (D) Flower growth rate by period, day versus night in wild-type and *RNAi:PhCHL* transgenic lines.

We analyzed the increase in flower length. Down regulation of *PhCHL* caused a strong decrease in flower growth speed in line 3 (Movie S2). The wild-type flowers had an overall growth speed that was always higher than in transgenic lines (Figure 4B). We calculated the differences in growth speed and found that the maximal slope indicating growth speed was 1.4-fold higher in wild type compared to transgenic line 3 (Table 2). We analyzed line 10, but due to flowering time differences, we were able to obtain data only from older flowers. These flowers also grew at a lower speed than wild type, but differences were not so pronounced (Movie S3) (Figure 4C).

Growth of hypocotyls in *Arabidopsis* is gated by the plant circadian clock [47]. We tested the hypothesis that petunia flowers may grow at different speeds during day and night. Indeed, we found that overall flower growth speed was higher during the day than during the night, coming to a sharp decrease in growth speed when flowers open (Figure 4D). The flowers corresponding to *RNAi:PhCHL* always grew slower than the wild types, but the time required to become fully developed was not affected by *PhCHL* (Figure 4D). Altogether, our data shows that *PhCHL* plays a role in organ growth speed and duration that is organ-specific.

### 3.7. *PhCHL* Coordinates Daily Changes in Scent Profiles

Petunia flowers emit mostly benzenoids/phenylpropanoids, including methyl benzoate, benzaldehyde and benzyl benzoate [48]. We also identified emission of terpenoids, cadinene and limonene. We selected 17 volatile organic compounds (VOCs) to analyze the effect of *PhCHL* silencing in volatile emission for a 24-hour period (Table 3). The major VOC emitted by *P. hybrida* was methyl benzoate (74.90% of selected volatiles) whereas cadinene was the volatiles with the lowest emission (0.02% of selected compounds). Methyl benzoate was also the principal emitted volatile in transgenic lines: 79.1% in *RNAi:PhCHL3* and 58.51% in *RNAi:PhCHL10* petunia flowers. The volatile with the lowest emission was acetophenone for *RNAi:PhCHL3* (0.01%) and cadinene for *RNAi:PhCHL10* (0.018%). Due to the high emission of methyl benzoate in all petunia lines, we analyzed the volatile profile excluding this compound (Figure 5, Figure S5A).

**Table 3.** Retention time (RT) expressed in minutes, name and CAS number (assigned by the Chemical Abstract Services) of selected volatiles.

| RT     | Name                    | CAS                |
|--------|-------------------------|--------------------|
| 4.873  | Benzaldehyde            | 100-52-7           |
| 6.435  | Limonene                | 138-86-3           |
| 6.539  | Benzyl alcohol          | 100-51-6           |
| 6.735  | Phenylacetaldehyde      | 122-78-1           |
| 7.230  | Acetophenone            | 98-86-2            |
| 7.825  | Methyl benzoate         | 93-58-3            |
| 8.149  | Phenylethyl alcohol     | 60-12-8            |
| 9.125  | Benzyl acetate          | 140-11-4           |
| 9.244  | Ethyl benzoate          | 93-89-0            |
| 9.668  | Methyl salicylate       | 119-36-8           |
| 10.720 | Phenylethyl acetate     | 103-45-7           |
| 12.287 | Eugenol                 | 97-53-0            |
| 12.711 | Benzyl 2-methylbutyrate | 56423-40-6         |
| 13.587 | Isoeugenol (isomers)    | 97-45-1; 5932-68-3 |
| 14.254 | Benzyl tiglate          | 37526-88-8         |
| 14.625 | Cadinene                | 483-76-1           |
| 17.525 | Benzyl benzoate         | 120-51-4           |

Excluding methylbenzoate (Figure S5A), the second-highest emitted volatile was ethyl benzoate in wild-type petunia and *RNAi:PhCHL10* line (45.72% and 48.61% of selected compounds, respectively). In contrast, the emission of ethyl benzoate was lower in *RNAi:PhCHL3* (10.23%) and the second major volatile in this transgenic line was isoeugenol (24.38%). Isoeugenol represented 15.84% in wild type and 10.92% in *RNAi:PhCHL10* (Figure 5A). We found that certain volatiles increased their emission in both

*RNAi:PhCHL* lines: benzaldehyde, phenylacetaldehyde, benzyl tiglate and benzyl 2-methylbutyrate (Figure 5A). The volatiles limonene, benzyl benzoate and acetophenone decreased their emission in *RNAi:PhCHL3* and *RNAi:PhCHL10* petunia flowers (Figure 5A) Finally, the quantities of some emitted volatiles varied among lines; the emission of benzyl acetate, cadinene, methyl salicylate, phenethyl acetate and phenethyl alcohol was higher in *RNAi:PhCHL3*, whereas the quantities of these compounds decreased in the *RNAi:PhCHL10* line (Figure 5A).

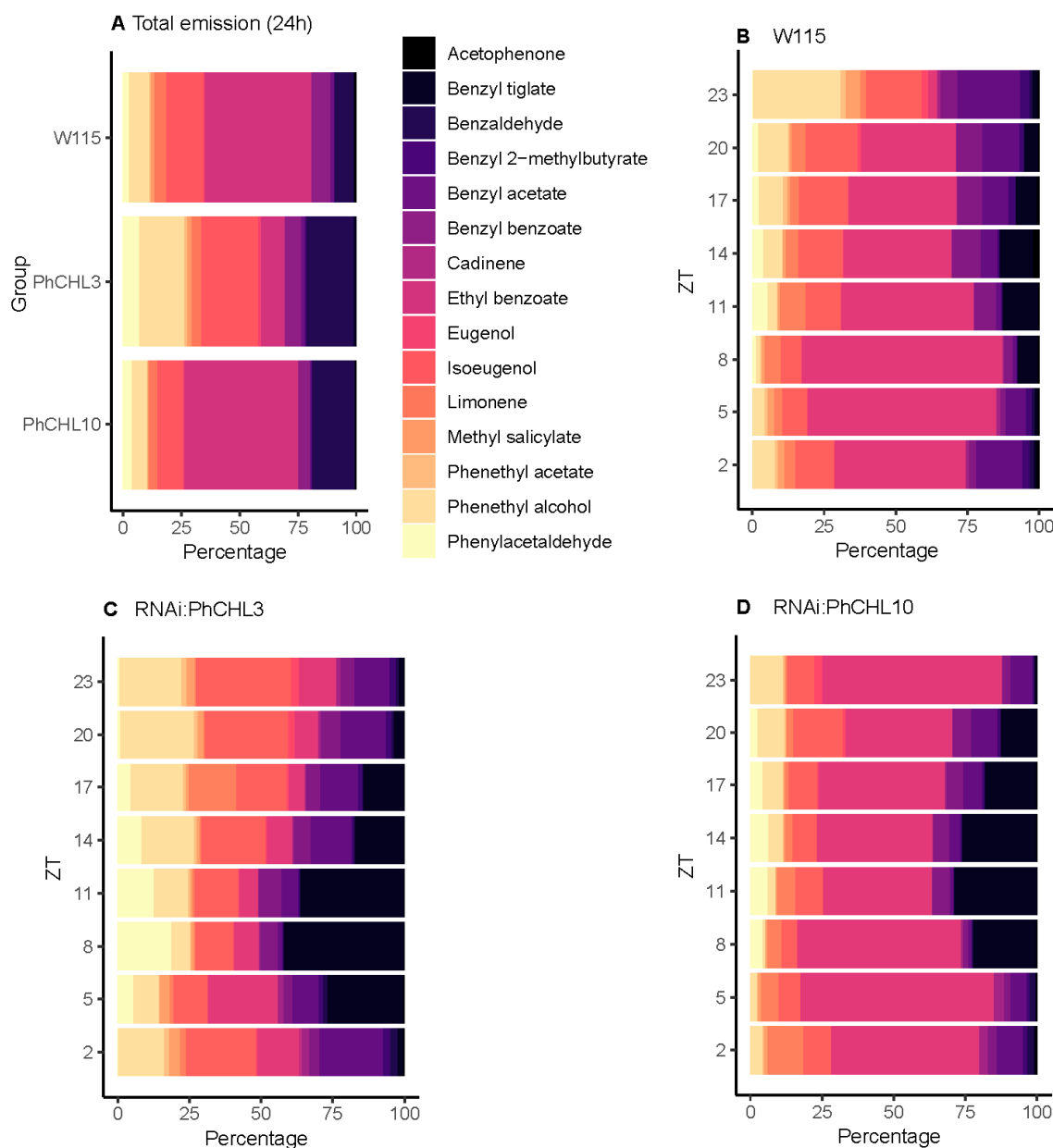


**Figure 5.** Petunia scent profiles expressed as percentage. Due to its high emission, methyl benzoate was excluded to visualize the remaining volatiles. Profiles were determined for 24 h emission under a 8L:16D cycle for the wild-type (first bar) and the transgenic lines (second and third bar) (A) and in a time-course (B–D), where each bar represent one sampling point (in ZT h) for wild-type (B), *RNAi:PhCHL3* (C) and *RNAi:PhCHL10* (D) petunia flowers.

As the quantitative changes in scent could occur at different times of the day, we collected scent every three h in an 8L:16D cycle. The profile analysis of floral compounds throughout 24 h revealed modifications in the contribution of single compounds to the scent profile.

Methyl benzoate was the major emitted compound by non-transgenic and transgenic petunia flowers. Its contribution to the floral scent varied from 69 to 79% in wild-type petunias, (Figure S5B), from 73 to 87% in RNAi line 3 (Figure S5C) and from 46% to 71% in RNAi line 10 (Figure S5D). Methyl benzoate tended to decrease during the light period in wild-type and *RNAi:PhCHL10* plants, in contrast in *RNAi:PhCHL3* the highest contribution to the floral scent occurred at ZT5 (Figure S5B–D).

As mentioned above, we excluded methyl benzoate to analyze the temporal variation in scent emission profiles of those volatiles with lower emission. Briefly, in the wild-type plants, benzyl 2-methylbutyrate contribution to the scent profile increased during the light period (ZT2, ZT5). Cadinene, had the highest contribution at dawn and transition to day light (ZT23–ZT2). In contrast, the VOCs benzaldehyde, ethyl benzoate, limonene and phenylacetaldehyde showed their major contribution to the scent composition at dusk and early night (ZT8, ZT11). Acetophenone and benzyl benzoate displayed their highest contribution to the flower aroma at midnight (ZT14, ZT17). Finally, benzyl alcohol, benzyl acetate, eugenol, isoeugenol, methyl salicylate, phenethyl alcohol and phenethyl acetate percent composition was higher at late night (ZT20, ZT23) (Figure 5B).

When we analyzed the floral scent composition in RNAi petunias, three types of changes in the scent profile were observed. A set of volatiles showed similar profiles to the wild type (Figure 5B–D). These included benzaldehyde, benzyl 2-methylbutyrate, cadinene, eugenol, isoeugenol and phenethyl alcohol. A second set of volatiles showed increased production during the late night and dawn (ZT23) as in wild type but did not decay during the light period (ZT2). Finally, acetophenone that had its maximal emission at midnight (ZT14–ZT17) and methyl salicylate (ZT20–ZT23) shifted their maxima to the light period at ZT2–ZT5.

These changes in timing of emission are reflected in the different quantitative combinations of VOCs found between wild-type and transgenic lines. Indeed, at the time when lights went off at ZT8, ethyl benzoate was the second important emitted volatile in W115 (70% of selected volatiles), decreasing in *RNAi:PhCHL10* to 57% and *RNAi:PhCHL3* to 8.7%. The VOCs acetophenone and phenethyl alcohol also decreased their emission in both transgenic lines. In contrast, benzaldehyde emission increased in both transgenic lines from 6.85% W115 (6.85%) to 41.8% in *RNAi:PhCHL3* and 22.1% in *RNAi:PhCHL10*. Phenylacetaldehyde also increased its emission in both *RNAi:PhCHL3* (18.7%) and *RNAi:PhCHL10* (4.3%) as petunia this volatile only represented a 1.4% of the profile in the wild-type (Figure 5B–D). When the lights went on at ZT0, scent also differed in transgenic and non-transgenic petunia flowers. The predominant compounds in the wild-type scent profile were phenethyl alcohol (30.5%), benzyl alcohol (21.9%) and isoeugenol (19.3%). In contrast, the major compounds in *RNAi:PhCHL3* were isoeugenol (33%), phenethyl alcohol (21.8%) ethyl benzoate (12.7%) meanwhile in *RNAi:PhCHL10* were ethyl benzoate (62.7%), phenethyl alcohol (11.4%) and isoeugenol (9.6%) (Figure 5B–D).

### 3.8. *PhCHL* Is Required for Timing of Scent Profiles

Petunia is considered a nocturnal plant; its scent emission is synchronized with pollinator activity. We analyzed the circadian rhythmicity of scent emission and the effect of silencing the gene *PhCHL*. In wild-type plants, benzaldehyde, benzyl acetate, benzyl alcohol, benzyl benzoate, eugenol, isoeugenol, methyl benzoate, phenylacetaldehyde, phenethyl acetate and phenethyl alcohol were rhythmically emitted ( $p < 0.05$ ), while acetophenone, benzyl 2-methylbutyrate, benzyl tiglate, cadinene, limonene, ethyl benzoate and methyl salicylate turned out to be arrhythmic ( $p > 0.05$ ) (Table 4). In the RNAi plants, most compounds emitted in a rhythmic fashion in wild type were emitted in a rhythmic manner (Table 4). Moreover, benzyl tiglate, benzyl 2-methylbutyrate and methyl salicylate were not rhythmically emitted both in W115 and *RNAi:PhCHL10* line oscillated significantly in *RNAi:PhCHL3* petunias (Table 4).

**Table 4.** Analysis of emitted volatiles with MetaCycle. The JTK\_CYCLE algorithm implemented in the R library “MetaCycle” was used to detect rhythms in emitted volatiles of petunia wild-type (W115) and transgenic *RNAi:PhCHL* lines (*PhCHL3*, *PhCHL10*). Volatiles with significant *p* value (*p* value < 0.05) showed a rhythmic emission. Phase is defined as the time point, in ZT h, with the highest emission.

| Volatile                | W115 <i>p</i> Value | Phase | PhCHL3 <i>p</i> Value | Phase | PhCHL10 <i>p</i> Value | Phase |
|-------------------------|---------------------|-------|-----------------------|-------|------------------------|-------|
| Benzyl tiglate          | 1.000               | 2     | 0.014                 | 0.5   | 0.476                  | 5     |
| Cadinene                | 0.445               | 5     | 0.246                 | 23    | 1.000                  | 9.5   |
| Ethyl benzoate          | 1.000               | 11    | 1.000                 | 20    | 1.000                  | 20    |
| Acetophenone            | 1.000               | 12.5  | 1.000                 | 8     | 0.210                  | 11    |
| Benzaldehyde            | 0.000               | 15.5  | 0.000                 | 12.5  | 0.000                  | 15.5  |
| Benzyl benzoate         | 0.001               | 15.5  | 0.023                 | 17    | 0.001                  | 17    |
| Limonene                | 0.165               | 15.5  | 0.280                 | 17    | 1.000                  | 11    |
| Phenylacetaldehyde      | 0.001               | 15.5  | 0.000                 | 12.5  | 0.000                  | 20    |
| Methyl benzoate         | 0.017               | 17    | 0.003                 | 15.5  | 0.011                  | 17    |
| Isoeugenol              | 0.001               | 18.5  | 0.007                 | 18.5  | 0.014                  | 17    |
| Benzyl acetate          | 0.003               | 20    | 0.001                 | 20    | 0.005                  | 20    |
| Eugenol                 | 0.001               | 20    | 0.000                 | 20    | 0.019                  | 20    |
| Methyl salicylate       | 1.000               | 20    | 0.009                 | 20    | 1.000                  | 15.5  |
| Phenylethyl acetate     | 0.048               | 20    | 0.002                 | 20    | 0.000                  | 20    |
| Phenylethyl alcohol     | 0.000               | 20    | 0.000                 | 18.5  | 0.000                  | 15.5  |
| Benzyl alcohol          | 0.000               | 21.5  | 0.007                 | 20    | 0.000                  | 20    |
| Benzyl 2-methylbutyrate | 1.000               | 23    | 0.011                 | 23    | 0.194                  | 2     |

We also analyzed the phase or time point with the highest emission of selected volatiles. Most compounds increased their emission during the dark period, and we classified the volatiles according to their maximum emission. In the wild-type petunia, first group comprised benzyl tiglate and cadinene, which showed their peaks during the subjective day (ZT2 and ZT5, respectively). The second group included the volatiles ethyl benzoate and acetophenone, that reached its maximum emission at early night (ZT11 and ZT12.5, respectively). The third group consisted of those VOCs which peaked at midnight, from ZT15 to ZT18.5: benzaldehyde, benzyl acetate, limonene, isoeugenol, methyl benzoate and phenylacetaldehyde. Finally, the fourth group included benzyl 2-methylbutyrate, benzyl acetate, benzyl alcohol, eugenol, methyl salicylate, phenethyl acetate and phenethyl alcohol, that showed their maximum emission at late night (ZT20 to ZT23) (Table 4).

Analyzing the phase of emitted volatiles in transgenic lines revealed important differences. We found four types of behavior. First, the volatiles benzyl acetate, eugenol and phenethyl acetate did not change their peak in wild-type and transgenic petunias (Table 4). Second, benzyl benzoate, cadinene and ethyl benzoate delayed their maximum emission in both transgenic lines (Table 4). Third, acetophenone, benzyl alcohol and phenethyl alcohol displayed an advanced phase in *RNAi:PhCHL* plants (Table 4). Finally, a group of volatiles did not follow the same pattern in *RNAi:PhCHL3* and *RNAi:PhCHL10* lines; benzyl 2-methylbutyrate and isoeugenol did not change their peak in *RNAi:PhCHL3* compared to W115 petunias whereas these compounds were emitted in advanced in the line *RNAi:PhCHL10*; on the other hand, the compounds benzaldehyde and methyl benzoate peaked at the same time in non-transgenic and *RNAi:PhCHL10* petunias but in the *RNAi:PhCHL3* line this peak was advanced (Table 4).

Altogether, *PhCHL* plays a fundamental role in coordinating floral scent profile of petunia that could be related to the timing of maximal production of different VOCs. The effect on single compounds appears to be opposite in some cases, suggesting a control of scent pathway at one of several points that we do not understand yet.

#### 4. Discussion

The *ZTL* gene in *Arabidopsis* plays a central role in the circadian clock regulation and affects several traits such as flowering time [45], and in *Nicotiana* it also controls flower daily movement and the emission of benzyl acetone [17]. Here we have performed a systematic study of *PhCHL*, the ortholog of *ZTL*, and its outputs in *Petunia hybrida*, uncovering several unreported functions.

The ZTL/FKF/LKP2 proteins are blue light receptors in Arabidopsis. The expression of ZTL is not rhythmic in Arabidopsis or *Nicotiana* [44,45]. While *PhCHL* showed a clear peak of expression in 12L:12D, we could not find a significant rhythm, indicating a conserved expression pattern with other plants where it has been analyzed. This is the first time that *PhCHL*, a ZTL ortholog, has been analyzed in petals. The similarity of expression of *PhCHL* in leaves and petals indicates that the leaf and petal clock may be partly conserved. However, this needs further analysis with more genes, as clock transcriptional structure has been shown to change in roots, pods or seeds [49,50].

One of the classical experiments in Chronobiology in plants was performed by d'Ortois de Mairan. He demonstrated that leaf movement was rhythmic and endogenous [51]. Leaf angle and leaf movement have been widely studied in crops, including soybean and maize [52,53] and in the canonical model Arabidopsis. The analysis of circadian clock mutants in Arabidopsis revealed that the clock genes *GIGANTEA* (*GI*) and *EARLY FLOWERING 4* (*ELF4*) are required to maintain leaf movement rhythmicity [54,55]. In petunia, we detected periodic changes in leaf position but diel changes in position were not affected by the down-regulation of *PhCHL*. This result suggests that *PhCHL* did not play a critical role in leaf rhythms at early stages of development.

The first apparent effect of down-regulating *PhCHL* was a decrease in plant body size. A detailed analysis using time lapse images showed that the stem of wild-type plants and siblings knocked down for *PhCHL* grew at similar speed. This suggests that the identified decrease in shoot length maybe the result of smaller primordia, decreased growth duration or a combination of both phenomena. In contrast, petal development appeared to be affected in growth rate. Furthermore, petal growth occurred at higher rates during the day than during the night both in wild-type and transgenic plants, suggesting that gated growth of flowers was independent of *PhCHL*. Work in Arabidopsis and maize has shown that the process of growth rate and duration maybe differentially affected by mutations [56–58]. Our results show that measuring two different organs may yield different results related to growth rate and duration. The plant circadian clock appears to have an organ specific resetting in roots, pods and seeds [50,59–61]. In this context, shoot growth is driven by the shoot apical meristem while flowers have undergone major organ identity reprogramming. As both cell division and expansion are under direct control of the clock [62,63], our results indicate a somewhat different interpretation of loss of *PhCHL* in stems and flowers.

We performed a complete scent profile analysis in wild-type and knockdown lines. Floral scent comprised 98.66% benzenoids/phenylpropanoids and 1.34% terpenoids in wild-type petunias. This composition was somewhat similar in transgenic lines, indicating that the effects of *PhCHL* are not specific for a single volatile family of compounds. The emission of several phenylpropanoids/benzenoids compounds, such as methyl benzoate, benzyl alcohol, benzyl benzoate or benzaldehyde, displayed a rhythmic oscillation whereas acetophenone or ethyl benzoate (phenylpropanoids/benzenoids) and the terpenoids cadinene and limonene did not. In addition, the amount of emitted volatiles tended to increase and peak during the dark phase, coinciding with petunia pollinators activity [64]. These results are similar to those described previously for whole flowers, indicating that petal volatiles and those emitted by other organs have similar control mechanism [14]. This suggests that the circadian clock plays a key role in the regulation of biosynthesis and emission of certain compounds that interacts and/or attracts pollinators. In contrast, volatiles which did not oscillate such as acetophenone, or terpenoids may play a role in defense [65,66].

The disruption of *PhCHL* shifted the maximum emission of benzyl alcohol was advanced whereas the peaks of benzyl benzoate and ethyl benzoate were delayed. Other volatiles, such as benzyl alcohol, eugenol and phenethyl acetate, were not affected by the knockdown of *PhCHL*. These results suggest that *PhCHL* was involved, directly or indirectly, in the emission pattern of certain volatiles. However complete knockouts for *PhCHL* may show a stronger effect in the volatiles affected and/or additional effects on those that appear to remain stable.

Flower fragrances play a complex biological role. The dominant nocturnal emitted volatiles of *Petunia axillaris*, benzaldehyde, benzyl alcohol and methyl benzoate, act as attractant of its nocturnal



pollinator [64] whereas benzaldehyde has been described as a mild repellent [67]. On the other hand, the highest emitted compound by *P. integrifolia* is benzaldehyde [64]. In *Petunia hybrida*, the three major compounds were methyl benzoate, ethyl benzoate and isoeugenol. In contrast, the three principal released VOCs in *RNAi:PhCHL3* were methyl benzoate, isoeugenol and benzaldehyde, while in *RNAi:PhCHL10*, they were methyl benzoate, ethyl benzoate and benzaldehyde. In addition, in the present work, we described how the proportion of the compounds emitted by wild-type and *RNAi:PhCHL* petunias changed throughout a 24 h period. Previous studies that covered the down-regulation of the clock genes *LHY* and *ZTL* in petunia and wild tobacco, have report a reduction in volatile emission and production [17,18]. Our results showed that silencing *PhCHL* modified blend ratios, resulting in a different scent profile. Changes in emission pattern and fragrance composition may have an effect in pollinator attraction, plant defense against herbivores and pathogens or plant-plant signaling [68–70]. Our work shows that *PhCHL* plays a major role in the quantities and timing of VOC emission, thus coordinating the proper composition and daily changes of scent blends.

**Supplementary Materials:** Supplementary materials are available online.

**Author Contributions:** M.I.T. designed experiments, performed experiments, performed formal data analysis, wrote, revised and edited the paper. F.P.S. designed experiments, developed the software, performed experiments, performed formal data analysis and revised and edited the paper. M.V.D.G. performed formal data analysis and revised and edited the paper. F.P.C. performed formal data analysis and revised and edited the paper. P.J.N. conceived and coordinated the study, designed experiments, developed the software, performed formal data analysis, revised and edited the paper, supervised this work and acquired funding. M.E.C. conceived and coordinated the study, designed experiments, performed formal data analysis, wrote, revised and edited the paper, supervised this work and acquired funding. J.W. conceived and coordinated the study, designed experiments, performed experiments, performed formal data analysis, revised and edited the paper, supervised this work and acquired funding. All authors revised and approved the final draft.

**Funding:** This research was funded by Fundación Seneca 19398/PI/14, 19895/GERM/15 and MC BFU-2017 88300-C2-1-R and BFU-2017 88300-C2-2-R.

**Acknowledgments:** We would like to acknowledge María José Roca for technical assistance.

**Conflicts of Interest:** The authors declare no conflict of interest. The funders had no role in the design of the study; in the collection, analyses, or interpretation of data; in the writing of the manuscript, or in the decision to publish the results.

## References

1. Barton, M.K. Twenty years on: The inner workings of the shoot apical meristem, a developmental dynamo. *Dev. Biol.* **2010**, *341*, 95–113. [[CrossRef](#)] [[PubMed](#)]
2. Angenent, G.C.; Immink, R.G.H.; Kaufmann, K. The “ABC” of MADS domain protein behaviour and interactions. *Semin. Cell Dev. Biol.* **2010**, *21*, 87–93.
3. Egea-Cortines, M.; Saedler, H.; Sommer, H. Ternary complex formation between the MADS-box proteins SQUAMOSA, DEFICIENS and GLOBOSA is involved in the control of floral architecture in *Antirrhinum majus*. *EMBO J.* **1999**, *18*, 5370–5379. [[CrossRef](#)] [[PubMed](#)]
4. Honma, T.; Goto, K. Complexes of MADS-box proteins are sufficient to convert leaves into floral organs. *Nature* **2001**, *409*, 525–529. [[CrossRef](#)] [[PubMed](#)]
5. Bernardello, G.; Anderson, G.J.; Stuessy, T.F.; Crawford, D.J. A survey of floral traits, breeding systems, floral visitors, and pollination systems of the angiosperms of the Juan Fernandez Islands (Chile). *Bot. Rev.* **2001**, *67*, 255–308. [[CrossRef](#)]
6. Hepworth, J.; Lenhard, M. Regulation of plant lateral-organ growth by modulating cell number and size. *Curr. Opin. Plant Biol.* **2014**, *17*, 36–42. [[CrossRef](#)] [[PubMed](#)]
7. Manchado-Rojo, M.; Weiss, J.; Egea-Cortines, M. Validation of *Aintegumenta* as a gene to modify floral size in ornamental plants. *Plant Biotechnol. J.* **2014**, *12*, 1053–1065. [[CrossRef](#)] [[PubMed](#)]
8. Krizek, B.A. Ectopic expression *Aintegumenta* in Arabidopsis plants results in increased growth of floral organs. *Dev. Genet.* **1999**, *25*, 224–236. [[CrossRef](#)]

9. Kuluev, B.; Avalbaev, A.; Nurgaleeva, E.; Knyazev, A.; Nikonorov, Y.; Chemeris, A. Role of AINTEGUMENTA-like gene NtANTL in the regulation of tobacco organ growth. *J. Plant Physiol.* **2015**, *189*, 11–23. [[CrossRef](#)] [[PubMed](#)]
10. Muhlemann, J.K.; Maeda, H.; Chang, C.Y.; Miguel, P.S.; Baxter, I.; Cooper, B.; Perera, M.A.; Nikolau, B.J.; Vitek, O.; Morgan, J.A.; et al. Developmental Changes in the Metabolic Network of Snapdragon Flowers. *PLoS ONE* **2012**, *7*, e40381. [[CrossRef](#)] [[PubMed](#)]
11. Manchado-Rojo, M.; Delgado-Benarroch, L.; Roca, M.J.; Weiss, J.; Egea-Cortines, M. Quantitative levels of Deficiens and Globosa during late petal development show a complex transcriptional network topology of B function. *Plant J.* **2012**, *72*, 294–307. [[CrossRef](#)] [[PubMed](#)]
12. Fenske, M.P.; Imaizumi, T. Circadian Rhythms in Floral Scent Emission. *Front. Plant Sci.* **2016**, *7*, 462. [[CrossRef](#)] [[PubMed](#)]
13. Dudareva, N.; Murfitt, L.M.; Mann, C.J.; Gorenstein, N.; Kolosova, N.; Kish, C.M.; Bonham, C.; Wood, K. Developmental regulation of methyl benzoate biosynthesis and emission in snapdragon flowers. *Plant Cell* **2000**, *12*, 949–961. [[CrossRef](#)] [[PubMed](#)]
14. Verdonk, J.C.; Ric de Vos, C.H.; Verhoeven, H.A.; Haring, M.A.; van Tunen, A.J.; Schuurink, R.C.; de Vos, C.H.R. Regulation of floral scent production in petunia revealed by targeted metabolomics. *Phytochemistry* **2003**, *62*, 997–1008. [[CrossRef](#)]
15. Hendel-Rahmanim, K.; Masci, T.; Vainstein, A.; Weiss, D. Diurnal regulation of scent emission in rose flowers. *Planta* **2007**, *226*, 1491–1499. [[CrossRef](#)]
16. Ruíz-Ramón, F.; Águila, D.J.; Egea-Cortines, M.; Weiss, J. Optimization of fragrance extraction: Daytime and flower age affect scent emission in simple and double narcissi. *Ind. Crops Prod.* **2014**, *52*, 671–678. [[CrossRef](#)]
17. Yon, F.; Joo, Y.; Cort, L.; Rothe, E.; Baldwin, I.T.; Kim, S.; Kim, S. Silencing *Nicotiana attenuata* LHY and ZTL alters circadian rhythms in flowers. *New Phytol.* **2015**, *203*, 1058–1066. [[CrossRef](#)]
18. Fenske, M.P.; Hewett-Hazelton, K.D.; Hempton, A.K.; Shim, J.S.; Yamamoto, B.M.; Riffell, J.A.; Imaizumi, T. Circadian clock gene LATE ELONGATED HYPOCOTYL directly regulates the timing of floral scent emission in *Petunia*. *Proc. Natl. Acad. Sci. USA* **2015**, *112*, 9775–9780. [[CrossRef](#)]
19. Bombarely, A.; Moser, M.; Amrad, A.; Bao, M.; Bapaume, L.; Barry, C.C.S.; Bliet, M.; Boersma, M.R.M.; Borghi, L.; Bruggmann, R.; et al. Insight into the evolution of the Solanaceae from the parental genomes of *Petunia hybrida*. *Nat. Plants* **2016**, *2*, 1–9. [[CrossRef](#)]
20. Birney, E.; Clamp, M.; Durbin, R. GeneWise and Genomewise. *Genome Res.* **2004**, *14*, 988–995. [[CrossRef](#)]
21. Larkin, M.A.; Blackshields, G.; Brown, N.P.; Chenna, R.; McGettigan, P.A.; McWilliam, H.; Valentin, F.; Wallace, I.M.; Wilm, A.; Lopez, R.; et al. Clustal W and clustal X version 2.0. *Bioinformatics* **2007**, *23*, 2947–2948. [[CrossRef](#)] [[PubMed](#)]
22. Paradis, E.; Claude, J.; Strimmer, K. APE: Analyses of Phylogenetics and Evolution in R language. *Bioinformatics* **2004**, *20*, 289–290. [[CrossRef](#)] [[PubMed](#)]
23. Schliep, K.P. Phangorn: Phylogenetic analysis in R. *Bioinformatics* **2011**, *27*, 592–593. [[CrossRef](#)]
24. Yu, G.; Smith, D.K.; Zhu, H.; Guan, Y.; Lam, T.T.-Y. Ggtree: An R package for visualization and annotation of phylogenetic trees with their covariates and other associated data. *Methods Ecol. Evol.* **2017**, *8*, 28–36. [[CrossRef](#)]
25. Helliwell, C.; Waterhouse, P. Constructs and methods for high-throughput gene silencing in plants. *Methods* **2003**, *30*, 289–295. [[CrossRef](#)]
26. Hilson, P.; Allemeersch, J.; Altmann, T.; Aubourg, S.; Avon, A.; Beynon, J.; Bhalarao, R.P.; Bitton, F.; Caboche, M.; Cannoot, B.; et al. Versatile gene-specific sequence tags for Arabidopsis functional genomics: Transcript profiling and reverse genetics applications. *Genome Res.* **2004**, *14*, 26–2189. [[CrossRef](#)] [[PubMed](#)]
27. Box, M.S.; Coustham, V.; Dean, C.; Mylne, J.S. Protocol: A simple phenol-based method for 96-well extraction of high quality RNA from Arabidopsis. *Plant Methods* **2011**, *7*, 7. [[CrossRef](#)]
28. Mallona, I.; Lischewsky, S.; Weiss, J.; Hause, B.; Egea-Cortines, M. Validation of reference genes for quantitative real-time PCR during leaf and flower development in *Petunia hybrida*. *BMC Plant Biol.* **2010**, *10*, 4. [[CrossRef](#)] [[PubMed](#)]
29. Pfaffl, M.W.; Tichopad, A.; Prgomet, C.; Neuvians, T.P. Determination of stable housekeeping genes, differentially regulated target genes and sample integrity: BestKeeper—Excel-based tool using pair-wise correlations. *Biotechnol. Lett.* **2004**, *26*, 509–515. [[CrossRef](#)] [[PubMed](#)]

30. Andersen, C.L.; Jensen, J.L.; Orntoft, T.F. Normalization of real-time quantitative reverse transcription-PCR data: A model-based variance estimation approach to identify genes suited for normalization, applied to bladder and colon cancer data sets. *Cancer Res.* **2004**, *64*, 5245–5250. [CrossRef]
31. Vandesompele, J.; De Preter, K.; Pattyn, F.; Poppe, B.; Van Roy, N.; De Paepe, A.; Speleman, F. Accurate normalization of realtime quantitative RT-PCR data by geometric averaging of multiple internal control genes. *Genome Biol.* **2002**, *3*, RESEARCH0034. [CrossRef] [PubMed]
32. Silver, N.; Best, S.; Jiang, J.; Thein, S.L. Selection of housekeeping genes for gene expression studies in human reticulocytes using real-time PCR. *BMC Mol. Biol.* **2006**, *7*, 33. [CrossRef] [PubMed]
33. Xie, F.; Xiao, P.; Chen, D.; Xu, L.; Zhang, B. miRDeepFinder: A miRNA analysis tool for deep sequencing of plant small RNAs. *Plant Mol. Biol.* **2012**, *80*, 75–84. [CrossRef] [PubMed]
34. Schmittgen, T.D.; Livak, K.J. Analyzing real-time PCR data by the comparative CT method. *Nat. Protoc.* **2008**, *3*, 1101–1108. [CrossRef]
35. Mallona, I.; Weiss, J.; Egea-Cortines, M. pcrEfficiency: A Web tool for PCR amplification efficiency prediction. *BMC Bioinform.* **2011**, *12*, 404. [CrossRef]
36. Navarro, P.J.; Pérez, F.; Weiss, J.; Egea-Cortines, M. Machine learning and computer vision system for phenotype data acquisition and analysis in plants. *Sensors* **2016**, *16*, 641. [CrossRef]
37. Kahm, M.; Hasenbrink, G.; Ludwig, J. Grofit: Fitting Biological Growth Curves with R. *J. Stat. Softw.* **2010**, *33*, 1–21. [CrossRef]
38. Ruiz-Hernández, V.; Roca, M.J.; Egea-Cortines, M.; Weiss, J. A comparison of semi-quantitative methods suitable for establishing volatile profiles. *Plant Methods* **2018**, *14*, 67. [CrossRef] [PubMed]
39. Hughes, M.E.; Hogenesch, J.B.; Kornacker, K. JTK\_CYCLE: An efficient nonparametric algorithm for detecting rhythmic components in genome-scale data sets. *J. Biol. Rhythm.* **2010**, *25*, 372–380. [CrossRef] [PubMed]
40. Wu, G.; Anafi, R.C.; Hughes, M.E.; Kornacker, K.; Hogenesch, J.B. MetaCycle: An integrated R package to evaluate periodicity in large scale data. *Bioinformatics* **2016**, *32*, 3351–3353. [CrossRef]
41. Wickham, H. *Ggplot2: Elegant Graphics for Data Analysis*; Springer: Berlin/Heidelberg, Germany, 2016; ISBN 978-3-319-24277-4.
42. Garnier, S.; Ross, N.; Rudis, B.; Sciaini, M.; Scherer, C. *Viridis: Default Color Maps from “Matplotlib”*; R Project: Vienna, Austria, 2018; R Package Version 0.5; Available online: <https://cran.r-project.org/web/packages/viridis/index.html> (accessed on 11 April 2019).
43. Kubota, A.; Kita, S.; Ishizaki, K.; Nishihama, R.; Yamato, K.T.; Kohchi, T. Co-option of a photoperiodic growth-phase transition system during land plant evolution. *Nat. Commun.* **2014**, *5*, 3668. [CrossRef] [PubMed]
44. Yon, F.; Seo, P.-J.; Ryu, J.Y.; Park, C.-M.; Baldwin, I.T.; Kim, S.-G. Identification and characterization of circadian clock genes in a native tobacco, *Nicotiana attenuata*. *BMC Plant Biol.* **2012**, *12*, 172. [CrossRef] [PubMed]
45. Somers, D.E.; Schultz, T.F.; Milnamow, M.; Kay, S.A. ZEITLUPE encodes a novel clock-associated PAS protein from *Arabidopsis*. *Cell* **2000**, *101*, 319–329. [CrossRef]
46. Navarro, P.J.; Fernández, C.; Weiss, J.; Egea-Cortines, M. Development of a configurable growth chamber with a vision system to study circadian rhythm in plants. *Sensors* **2012**, *12*, 15356–15375. [CrossRef] [PubMed]
47. Nusinow, D.A.; Helfer, A.; Hamilton, E.E.; King, J.J.; Imaizumi, T.; Schultz, T.F.; Farré, E.M.; Kay, S.A.; Farre, E.M. The ELF4-ELF3-LUX complex links the circadian clock to diurnal control of hypocotyl growth. *Nature* **2011**, *475*, 398. [CrossRef] [PubMed]
48. Amrad, A.; Moser, M.; Mandel, T.; de Vries, M.; Schuurink, R.C.; Freitas, L.; Kuhlemeier, C. Gain and Loss of Floral Scent Production through Changes in Structural Genes during Pollinator-Mediated Speciation. *Curr. Biol.* **2016**, *26*, 3303–3312. [CrossRef] [PubMed]
49. Endo, M. Tissue-specific circadian clocks in plants. *Curr. Opin. Plant Biol.* **2016**, *29*, 44–49. [CrossRef]
50. Weiss, J.; Terry, M.I.; Martos-Fuentes, M.; Letourneux, L.; Ruiz-hernández, V.; Fernández, J.A.; Egea-cortines, M. Diel pattern of circadian clock and storage protein gene expression in leaves and during seed filling in cowpea (*Vigna unguiculata*). *BMC Plant Biol.* **2018**, *18*, 33–53. [CrossRef]
51. De Mairan, J.-J. *Observation Botanique; Histoire de l’Académie Royale des Sciences Paris; Institut de France: Paris, France, 1729*; p. 35.
52. Ku, L.; Wei, X.; Zhang, S.; Zhang, J.; Guo, S.; Chen, Y. Cloning and Characterization of a Putative TAC1 Ortholog Associated with Leaf Angle in Maize (*Zea mays* L.). *PLoS ONE* **2011**, *6*, e20621. [CrossRef] [PubMed]

53. Kao, W.-Y.; Tsai, T.-T. Tropic leaf movements, photosynthetic gas exchange, leaf  $\delta^{13}\text{C}$  and chlorophyll a fluorescence of three soybean species in response to water availability. *Plant Cell Environ.* **1998**, *21*, 1055–1062. [[CrossRef](#)]
54. Park, D.H. Control of Circadian Rhythms and Photoperiodic Flowering by the Arabidopsis GIGANTEA Gene. *Science* **1999**, *285*, 1579–1582. [[CrossRef](#)] [[PubMed](#)]
55. Doyle, M.R.; Davis, S.J.; Bastow, R.M.; McWatters, H.G.; Kozma-Bognar, L.; Nagy, F.; Millar, A.J.; Amasino, R.M. The ELF4 gene controls circadian rhythms and flowering time in Arabidopsis thaliana. *Nature* **2002**, *419*, 74–77. [[CrossRef](#)] [[PubMed](#)]
56. Kennaway, R.; Coen, E.; Green, A.; Bangham, A. Generation of diverse biological forms through combinatorial interactions between tissue polarity and growth. *PLoS Comput. Biol.* **2011**, *7*, e1002071. [[CrossRef](#)]
57. Beemster, G.T.S.; De Vusser, K.; De Tavernier, E.; De Bock, K.; Inze, D. Variation in growth rate between Arabidopsis ecotypes is correlated with cell division and A-type cyclin-dependent kinase activity. *Plant Physiol.* **2002**, *129*, 854–864. [[CrossRef](#)]
58. Feys, K.; Demuyne, K.; De Block, J.; Bisht, A.; De Vlieghe, A.; Inzé, D.; Nelissen, H. Growth rate rather than growth duration drives growth heterosis in maize B104 hybrids. *Plant Cell Environ.* **2017**, *41*, 374–382. [[CrossRef](#)] [[PubMed](#)]
59. Thain, S.C.; Murtas, G.; Lynn, J.R.; McGrath, R.B.; Millar, A.J. The circadian clock that controls gene expression in Arabidopsis is tissue specific. *Plant Physiol.* **2002**, *130*, 102–110. [[CrossRef](#)] [[PubMed](#)]
60. Bordage, S.; Sullivan, S.; Laird, J.; Millar, A.J.; Nimmo, H.G. Organ specificity in the plant circadian system is explained by different light inputs to the shoot and root clocks. *New Phytol.* **2016**, *212*, 136–149. [[CrossRef](#)] [[PubMed](#)]
61. Voß, U.; Wilson, M.H.; Kenobi, K.; Gould, P.D.; Robertson, F.C.; Peer, W.A.; Lucas, M.; Swarup, K.; Casimiro, I.; Holman, T.J.; et al. The circadian clock rephases during lateral root organ initiation in Arabidopsis thaliana. *Nat. Commun.* **2015**, *6*, 7641. [[CrossRef](#)] [[PubMed](#)]
62. Farré, E.M. The regulation of plant growth by the circadian clock. *Plant Biol.* **2012**, *14*, 401–410. [[CrossRef](#)]
63. Fung-Uceda, J.; Lee, K.; Seo, P.J.; Polyn, S.; De Veylder, L.; Mas, P. The Circadian Clock Sets the Time of DNA Replication Licensing to Regulate Growth in Arabidopsis. *Dev. Cell* **2018**, *45*, 101–113. [[CrossRef](#)] [[PubMed](#)]
64. Hoballah, M.E.; Stuurman, J.; Turlings, T.C.J.; Guerin, P.M.; Connétable, S.; Kuhlemeier, C.; Connetable, S.; Kuhlemeier, C. The composition and timing of flower odour emission by wild *Petunia axillaris* coincide with the antennal perception and nocturnal activity of the pollinator *Manduca sexta*. *Planta* **2005**, *222*, 141–150. [[CrossRef](#)] [[PubMed](#)]
65. Unsicker, S.B.; Kunert, G.; Gershenzon, J. Protective perfumes: The role of vegetative volatiles in plant defense against herbivores. *Curr. Opin. Plant Biol.* **2009**, *12*, 479–485. [[CrossRef](#)]
66. Pichersky, E.; Gershenzon, J. The formation and function of plant volatiles: Perfumes for pollinator attraction and defense. *Curr. Opin. Plant Biol.* **2002**, *5*, 237–243. [[CrossRef](#)]
67. Junker, R.R.; Blüthgen, N. Floral scents repel potentially nectar-thieving ants. *Evol. Ecol. Res.* **2008**, *10*, 295–308.
68. Aharoni, A. Terpenoid Metabolism in Wild-Type and Transgenic Arabidopsis Plants. *Plant Cell Online* **2003**, *15*, 2866–2884. [[CrossRef](#)] [[PubMed](#)]
69. Yon, F.; Kessler, D.; Joo, Y.; Cortés Llorca, L.; Kim, S.G.; Baldwin, I.T. Fitness consequences of altering floral circadian oscillations for *Nicotiana attenuata*. *J. Integr. Plant Biol.* **2017**, *59*, 180–189. [[CrossRef](#)] [[PubMed](#)]
70. Bhatia, V.; Maisnam, J.; Jain, A.; Sharma, K.K.; Bhattacharya, R. Aphid-repellent pheromone E- $\beta$ -farnesene is generated in transgenic Arabidopsis thaliana over-expressing farnesyl diphosphate synthase2. *Ann. Bot.* **2015**, *115*, 581–591. [[CrossRef](#)] [[PubMed](#)]

